Visualization of an Endogenous Mitochondrial Azoreductase Activity under Normoxic Conditions Using a Naphthalimide Azo-Based Fluorogenic Probe

Laurane Michel, Marie Auvray, Laurie Askenatzis, Marie-Ange Badet-Denisot, Jérôme Bignon, Philippe Durand, Florence Mahuteau-Betzer, Arnaud Chevalier

Visualization of an endogenous mitochondrial azoreductase activity under normoxic conditions using a naphthalimide azo-based fluorogenic probe.

Laurane Michel[a], Dr. Marie Auvray[b,c], Laurie Askenatzis[a], Dr. Marie-Ange Badet-Denisot[a], Jérôme Bignon[a], Dr. Philippe Durand[a], Dr. Florence Mahuteau-Betzer[b,c], and Dr. Arnaud Chevalier[a]*.

a. Université Paris-Saclay, CNRS, Institut de Chimie des Substances Naturelles, UPR 2301, 91198, Gif-sur-Yvette, France.

b. CNRS UMR 9187, Inserm U1196 Chemistry and Modeling for the Biology of Cancer Institut Curie,Université PSL, 91400 Orsay (France).

c. CNRS UMR 9187, Inserm U1196 Chemistry and Modeling for the Biology of Cancer , Université Paris-Saclay, 91400 Orsay (France).

*Email: arnaud.chevalier@cnrs.fr

ABSTRACT: In this article, we demonstrate the existence of an endogenous mitochondrial azoreductase (AzoR) activity that can induce the cleavage of N=N double bonds of azobenzene compounds under normoxic conditions. To this end, 100% OFF-ON azo-based fluorogenic probes derived from 4-amino-1,8-naphthalimide fluorophores have been synthesized and evaluated. The *in vitro* study conducted with other endogenous reducing agents of the cell, including reductases, demonstrated both the efficacy and the selectivity of the probe for AzoR. Confocal experiments with the probe revealed an AzoR activity in the mitochondria of living cells under normal oxygenation conditions, and we were able to demonstrate that this endogenous AzoR activity appears to be expressed at different levels across different cell lines. This discovery provides crucial information in our understanding of the biochemical processes occurring within the mitochondria. It thus contributes to a better understanding of its function, which is implicated in numerous pathologies.

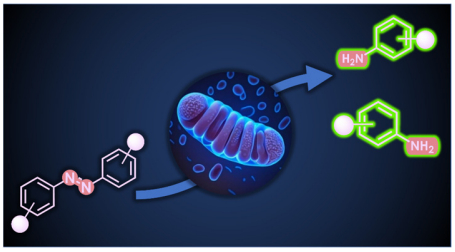

INTRODUCTION

The mitochondrion is the energy center of the cell. Because of its central role in the effective function of the cell, its dysfunction is linked with a variety of pathologies.[1] This organelle plays a key role in the development of multiple cancers[2-4] and neurodegenerative diseases[5-8]. More recently, the role of mitochondria has also been demonstrated in the development of diabetes[9] or non-alcoholic hepatic steatosis[10], which are regrettably increasingly prevalent around the world and will represent major public health issues in the coming years. Mitochondrial dysfunction can also result in cardiovascular disorders[11] and was recently demonstrated to be involved in cardiac failure in COVID-19 patients.[12] The observation of this organelle is therefore particularly relevant to improve our understanding of its functioning and thereby prevent any potential dysfunction. For decades now, a growing number of tools have been dedicated to the observation of mitochondria using fluorescence imaging. Murphy demonstrated that a lipophilic cation could be used to vectorize a given molecule into the mitochondrial matrix, taking advantage of the mitochondrial membrane potential.[13-14] Although the generality of this approach remains to be demonstrated, an ever-increasing number of articles describe successful uses of cationic units such as triphenylphosphonium (TPP)[15] for the delivery of a wide range of agents (fluorescent probes or drugs).[16-17] Numerous fluorogenic probes have been designed, enabling the observation of a wide range of intramitochondrial biological processes.[18-20] In this context, recent interest has emerged in the visualization of enzymatic activities, in particular reductases. The role of some of them remains unclear; also we can plausibly speculate that they are essential modulators in maintaining the redox equilibrium of the mitochondrial machinery.[21-24] The first evidence of such activity dealt with mitochondrial thioredoxin reductase activity.[25-28] We have also demonstrated the presence of a mitochondrial nitroreductase (NTR) activity capable of reducing the nitro function to the corresponding amine under normoxic conditions.[29] Several applications have followed using this mitochondrial NTR[30-34] such as two-color, three-dimensional, single-molecule fluorescence microscopy[31], proximity-based protein labeling[34], or activatable prodrugs for mitochondrial redox homeostasis disruption.[35] More recently, quinone reductases[36-38] and methionine reductase[39] activities have also been reported. To the best of our

knowledge, no fluorogenic probe has so far demonstrated any mitochondrial azoreductase (AzoR) activity in normoxic conditions. AzoR enables the breaking of the N=N double bond of an azobenzene unit thereby separating the two constituent parts by producing the corresponding anilines. This activity has mainly been observed in bacterial cultures by monitoring the decolorization of azo dyes.[40] Fluorogenic detection of AzoR-mediated reduction of azobenzene-modified fluorophores has also been implemented in this context.[41-43] In mammalian cells, this AzoR activity is mainly considered to be sensitive to oxygen and has therefore often been used as a marker of cellular hypoxia.[44-48] By analogy with our previous results on NTR, we consider the visualization of mitochondrial AzoR activity under normal oxygenation conditions. To our knowledge, this activity has never been reported under such conditions.

EXPERIMENTAL SECTION

Synthesis of Compound 4a. $NOBF_4$ (6.70 mg, 57.4 mmol, 1.10 eq.) was slowly added to a cooled solution of compound **2a** (14.0 mg, 52.2 µmol, 1.00 eq.) in of dry CH_3CN (2.00 mL) and stirred under argon at 0 °C for 30 min. After completion of the reaction (monitored by TLC), a solution of *N,N*-dimethylaniline (7.90 µL, 62.6 µmol, 1.20 eq.) in dry CH_3CN (500 µL) was slowly added dropwise. The reacting mixture was allowed to warm to room temperature and then stirred for another hour. The mixture was diluted in CH_2Cl_2 (20.0 mL) and washed with saturated aqueous NH_4Cl solution (3 x 10.0 mL). Organic phase was dried over $MgSO_4$ and solvents were evaporated under reduced pressure. The residue was purified by chromatography on silica gel (Hept/EtOAc, 85/15, v/v), giving **4a** as a dark purple solid (11.2 mg, 53%). ^{1}H NMR (500 MHz, $CDCl_3$) δ 9.23 (d, *J* = 8.3 Hz, 1H), 8.65 (t, *J* = 7.2 Hz, 2H), 8.04 (d, *J* = 9.1 Hz, 2H), 7.96 (d, *J* = 8.0 Hz, 1H), 7.83 (t, *J* = 7.8 Hz, 1H), 6.80 (d, *J* = 9.1 Hz, 2H), 4.21 (t, *J* = 7.4 Hz, 2H), 3.16 (s, 6H), 1.74 (qt, J = 7.4 Hz, 2H), 1.47 (sx, *J* = 7.5 Hz, 2H), 0.99 (t, *J* = 7.4 Hz, 3H). ^{13}C NMR (126 MHz, $CDCl_3$) δ 164.5, 164.1, 153.4, 151.9, 144.7, 131.8, 131.3, 130.6, 129.3, 129.2, 126.7, 126.4 (2C), 122.6, 122.1, 112.3, 111.6 (2C), 40.3, 40.3 (2C), 30.3, 20.4, 13.8. HRMS (ESI-MS) m/z: [M + H]+ Calcd for $C_{24}H_{25}N_4O_2$ 401.1974, found 401.1978.

General procedure for the synthesis of azo-based probe 4b-d through Path A. $NaNO_2$ (1.10 eq.) was added to a cooled 0.5 M HCl(aq) solution (400 µL) at 0 °C and the resulting mixture was stirred for 1 hour. A solution of ANI-based fluorophore **2** (1.00 eq.) in CH_3CN (100 µL) was added slowly dropwise and the resulting mixture was stirred at 0 °C until complete formation of diazonium salt (monitored by TLC). A solution of *N,N*-dimethylaniline (1.2 eq.) in CH_3CN (1.00 mL) was then slowly added at 0 °C. The reaction medium was then allowed to warm to room temperature and stirred for another 2 h. After completion of the reaction mixture, it was diluted in DCM (10.0 mL), washed with NH_4Cl aqueous sat. solution (3 x 10.0 mL). The organic phase was dried over $MgSO_4$, and the solvent was removed by evaporation under reduced pressure. The residue was purified by chromatography on silica gel. When reversed phase purification was needed, the mixture was directly diluted in water (2.00 mL) then purified by C18-reverse phase silica gel column chromatography using appropriate eluting solvent mixture to afford the desired pure product. All data relating to the preparation and purification of probes **4b-d** including compounds characterization are available in Supporting Information

General Procedure for the synthesis of azo-based probe 4e-f through Path B. To a suspension of 6-((4-(dimethylamino)phenyl)diazenyl)-1H,3H-benzo[de]isochromene-1,3-dione (**3**) (1.00 eq.) in absolute EtOH (0.1 M) was added corresponding amine (2.00 eq.). The resulting reaction mixture was heated at 90 °C overnight. After the reaction was completed (monitored by TLC), the reaction mixture was cooled to room temperature and the solvents were evaporated under reduced pressure. The residue was purified by flash chromatography on silica gel or by C18-reverse phase silica gel column chromatography, using an appropriate eluting solvent mixture to afford the desired pure product. All data relating to the preparation and purifications of probe **4e-f** including compounds characterization are available in supporting information

In vitro enzymatic activation assays. Kinetics assays were performed using a SpectraMax iD3 plate reader at 37°C. A stock solution of 50 mM potassium phosphate buffer pH 7.7 with 5% glycerol was made. This stock solution was used as buffer for all the test performed in 96 Well Costar Flat Bottom assay plates for fluorescence assays and 96 Well Greiner Bio-One ELISA Microlon® 200 microplates for absorbance assays. Enzyme were solubilized and stocked in 10% glycerol, 50.0 mM potassium phosphate buffer pH 7.7, at -80°C. 2.00 mM of DTT was added in the case of NQO1 and NQO2 stock solutions. Reactions were initiated by the addition of enzyme. The final assay solution contained a total volume of 200 µL. All assays have been performed in triplicate. Time-dependent fluorescence measurements were carried out to monitor release of the free fluorophore 2 (λ_{Ex} = 430 nm and λ_{Em} = 540 nm). Background measurements were taken in the absence of enzyme or reducers for each assay, also in triplicate. Background values were subtracted from the values obtained in presence of enzyme/reducers

Cell Culture. Human cancer cell lines were obtained from the American type Culture Collection (ATCC, Rockville, USA) and were cultured according to the supplier's instructions. U87-MG glioblastoma and Mia-Paca-2 pancreatic carcinoma cells were grown in Dulbecco minimal essential medium (DMEM) containing 4.50 g/L glucose supplemented with 10% FCS and 1% glutamine. MCF7 breast carcinoma, K562 myelogenous leukemia, A549 lung carcinoma and HeLa cervical carcinoma cells were grown in RPMI 1640 containing 10% FCS and 1% glutamine. HCT116 colorectal carcinoma cells were grown in McCoy containing 4.50 g/L glucose supplemented with 10% FCS and 1% glutamine. All cell lines were maintained at 37 °C in a humidified atmosphere containing 5% CO2. For live cells fluorescence microscopy, an Ibidi® µSlide 8 Well high Glass Bottom plate was seeded with 15 000 cells/well and then maintained at 37 °C in a humidified atmosphere containing 5% CO2 for 24h to 48h.

Confocal Microscopy. Fluorescence images were acquired using a Leica SP8-X inverted confocal microscope with a 63× oil immersion objective (HC PL APO CS2 Leica). Excitation was performed using a White light laser pulsed at 80MHz and a Diode 440 nm LDH-P-C-440B pulsed at 40 MHz. Detection was carried out by using PMT detector (Hamamatsu 6357) collecting photons, or GaAsP Hybrid (Hamamatsu) collecting photons over the appropriate emission wavelength window as specified in the figures captions.

RESULTS AND DISCUSSION

For this purpose, we have synthesized a series of naphthalimide-based fluorophores. This dye is commonly used in fluorescence microscopy since its photophysical properties are compatible with cell imaging (good QY, green emission). Its main advantage lies in the presence of the aniline, which constitutes a functionalizable fluorogenic center to design responsive sensors.[49-50] Furthermore, the alkylation of the imide nitrogen constitutes an easy way to modulate its physicochemical properties, such as water solubility, or its mitochondria-targeting ability. In addition to the commonly used butyl naphthalimide, we synthesized a set of fluorophores with various R substituents. Besides the fluorophores described in part in the literature,[51-53] we included two original structures. ANI **2c** features a pyridinium group, providing both water solubility and mitochondrial targeting ability.

Scheme 1. Synthesis of 4-ANI fluorophores (**2a-f**) and corresponding azo-based probes (**4a-f**). [a]Method A was used for the preparation of the diazonium salt. [b]Method B was used for the preparation of diazonium salt. [c]Probe obtained from anhydride 3

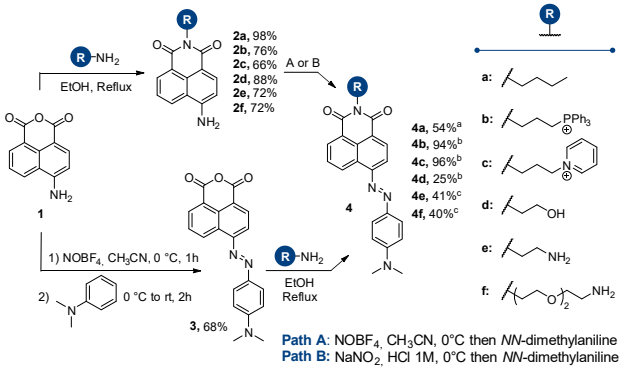

Fluorophore **2f**, on the other hand, constitutes a non-targeted analog with enhanced aqueous solubility thanks to the presence of the PEG2-amine moiety. Azobenzene derivatives of naphthalimides have almost never been reported in the literature. A single article documents the spectrophotometric properties of aryl-azo derivatives of naphthalimides, with a lack of details regarding their synthesis.[54] We thus designed a synthetic route to such compounds (Scheme 1).The 4-arylazo-1,8-naphthalimides **4a-d** were obtained from the 4-Amino-1,8-naphthalic anhydride **1** through either first the formation of the imides **2**, followed by that of the azo bound or in the reverse order *via* the 4-azo anhydride **3.** The azo bond was formed by a two steps process involving first the synthesis of a diazonium salt that can be achieved using two methods (Path A or Path B), followed by a SE_{Ar} reaction of *N,N*-dimethylaniline. The first strategy was found more efficient and more convenient for the 4-arylazo-1,8-naphthalimides **4a-d** while the second was preferred for the preparation of probes **4e** and **4f** carrying a primary amine on the R chain that could interfere with the nitrosylation agent All ANI fluorophores (**2a-f**) and corresponding azo-based probes (**4a-f**) were fully characterized and their structure was unambiguously confirmed by a set of structural analyses including NMR and HRMS (all data are accessible in the Sup Info file). We then proceeded with the photophysical characterization of all fluorophores (**2a-f**) and corresponding azo-based probes (**4a-f**) (See Tables S1 and S2). As expected, the measurements confirmed the complete absence of fluorescence from azo compounds **4a-g** (Cf Figure. S1-S2). This absence of fluorescence is mainly due to the prominence of the nonradiative deactivation related to photochemical isomerization or a rotation mechanism around the N=N double bond.[55] This characteristic of azobenzenes justifies their use in the design of fluorogenic sensors.[47] Also, a non-radiative and unreactive nπ* pathway has recently been claimed as a possible quenching mechanism of azobenzenes.[56] Azo-based compounds **4a-f** display a broad absorbance spectrum covering blue–orange (ca. 450–600 nm) part of the visible spectrum with an absorption maximum centered at around 535 nm in DMSO (Cf. Figure S5).

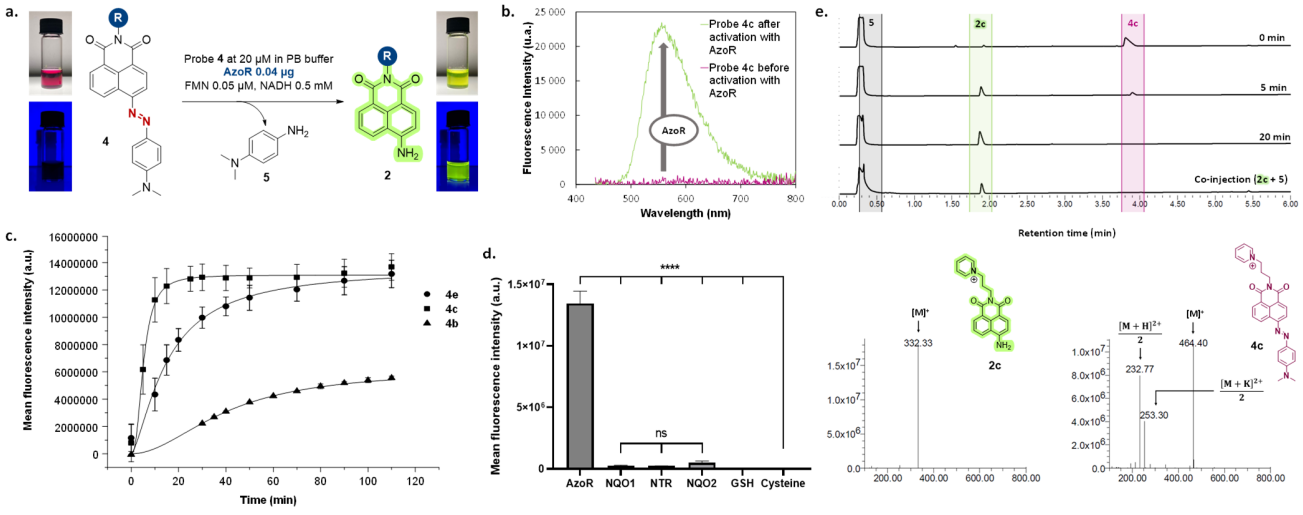

Figure 1. **In vitro study of Azo-based probes activation by AzoR. a.** Schematic representation of enzymatic reaction with pictures reflecting the color change of the solution (top vials) and the green fluorescence emission appearance with activation by AzoR (bottom vials). **b.** Emission spectra (λExc = 430 nm) of probe **4c** were recorded at 37 °C in PB buffer before and after 2h of activation by AzoR. **c**. Kinetic monitoring of AzoR activation of probes **4b**, **4c** and **4e**, the fluorescence was recorded over time at 540 nm with excitation fixed at 420 nm. **d.** Comparison of fluorescence intensity recorded after 30 min of incubation with multiple reducing agents at 37 °C (see supporting information). **e.** UPLC-MS chromatograms of the AzoR-mediated transformation of probe **4c** giving corresponding fluorophore **2c** together with aniline **5.** MS spectra of the peaks detected on the UPLC-MS chromatograms corresponding to the compounds **2c** and **4c**

A hypsochromic shift of the absorbance maximum was observed in PBS (Table S1 and Figure S6), that might be attributed to an aggregation of these compounds in aqueous media. This hypothesis seems plausible in the view of additional measurements in PBS containing 5% BSA, used here as a surfactant to avoid aggregation.[57] They displayed red-shifted absorbance spectra (Cf Figure. S7) close to those measured in DMSO, together with a substantial increase in the molar extinction coefficient that reflects a much better solubility (Table S1). However, the absorbance spectra of azo probes **4b**, **4c,** and **4e** in PBS buffer remain very similar to those measured in DMSO, with no requirement for supplementation with BSA, attesting to their suitable water solubility for use in biological media. We also evaluated the fluorescence properties of fluorophores **2a-f.** Overall, comparable values were observed for the majority of fluorophores (Cf. Table S2). Absorption maxima were located around 438 nm in DMSO, with green emission recorded between 550 and 560 nm. Fluorescence quantum yields appeared more irregular, fluctuating between 0.14 and 0.62, the lowest values being associated with the most lipophilic compounds. However, these values remain relatively acceptable for fluorescence imaging purposes. In PBS buffer, QY values drop as expected, but still provide acceptable brightness values for use in confocal microscopy (All spectra are present in Figures. S3-S4). Also note that fluorophore **2c** exhibited quite good resistance to photobleaching as more than 60% of residual signal was observed after 2h of irradiation at 300 mW.cm^{-2} (Cf. Figure. S9). We then assessed the turn-on response efficiency of our probes toward azoreductase. The AzoR was produced from *E. Coli*.[58] Tagged AzoR (EcAzoR-His6) was overexpressed in a culture of Rosetta (DE3) E. coli cells harboring pMAD600, then purified and isolated for *in vitro* activation assays (See Supporting Information for more details). The AzoR activity was first checked by monitoring the reduction of methyl red as a model substrate (See Figure. S10). We then investigated its action on fluorogenic probes **4a-f**. Figure 1c depicts the kinetic monitoring results obtained with probes **4b**, **4c** and **4e** which were found to be the most soluble in aqueous media. Each probe features an increase in fluorescence intensity at 530 nm over time, reflecting the formation of the ANI fluorophores and therefore the azoreductase-mediated reduction of the N=N double bond. The total absence of fluorescence of the azobenzene probes, leads to a considerable exaltation factor after AzoR-mediated activation, as we can see in Figure 1b. This constitutes an obvious benefit of this fluorogenic detection strategy. Note that the most efficient probe is the pyridinium-substituted azo-based probe **4c** for which a plateau is reached within 20 min. The activation of the TPP derived probe **4b** is less straightforward. This can be in part explained by its lower solubility limiting its effective concentration, but also by partial enzyme inhibition caused by the released fluorophore **2b.** Indeed, inhibition of AzoR-mediated reduction of methyl red was observed in the presence of fluorophore **2b** (See Figure. S11a), whereas no such effect was witnessed using fluorophore **2c** (See Figure. S11b) or *p*-dimethyl amino aniline **5** (See Figure. S11c). This result further justifies the design of original fluorophores, such as pyridinium-ANI **2c** in this case, which is more soluble and less inhibitory than fluorophore **2b**, while maintaining effective mitochondrial targeting. All the other tested probes were not activated *in vitro* by AzoR (data not shown). Considering the excellent response efficiency of probe **4c**, we evaluated its selectivity for AzoR by exposing it to other potent endogenous reducing agents (Figure 1d). After checking their effective activity on models substrates (Cf Figure. S12), nitroreductase (NTR) and quinone reductases (NQO1 and NQO2) were tested, as well as biothiols such as glutathione and cysteine that are highly present in cells and reported in the literature as able to reduce azobenzene.[59]

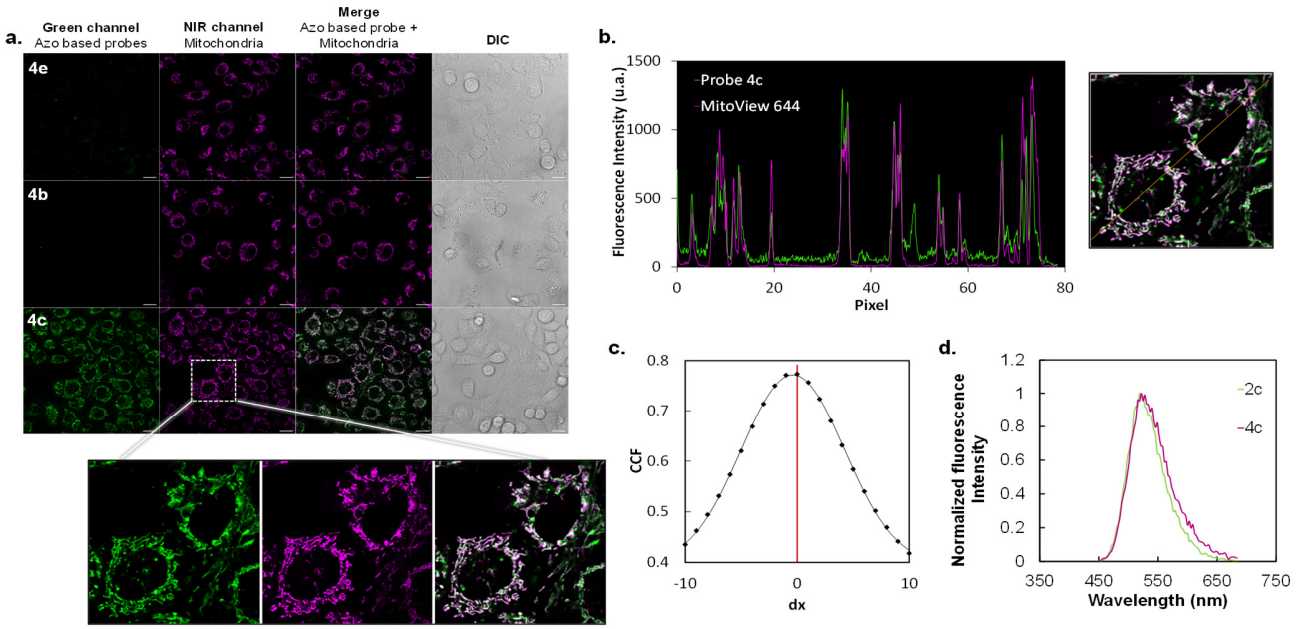

Figure 2. Confocal microscopy experiments reveal an endogenous mitochondrial AzoR in live cells. a. Confocal microscopy experiments with azo-based probes **4b**, **4c** and **4e** incubated with A459 live cells for 3h at 0.5 µM (λExc: 440 nm, λEm: 450 to 600 nm) in the presence of MitoView^{TM} 633 at 0.1 µM for 15 min (λExc: 630 nm, λEm: 650 to 750 nm), Scale Bar 20 µm. b. Plot profile of probe **2c** and of MitoView 633^{TM} recorded using the JAcOP plugin of ImageJ. c. Colocalization analysis using Van Steensel Cross-correlation functions (CCFs) demonstrating strong co-localization of **4c** and MitoView^{TM} 633 fluorescent signals (using JAcOP plugin of ImageJ). d. Overlap of emission spectra of fluorophore **2b** and activated azo-based probe **4c** recorded in live cell mitochondria.

To our delight, none of the tested reducers demonstrated any significant action after 30 min incubation (Figure 1d), a time at which the plateau is reached with AzoR. This indicates a high selectivity of probe **4c** for AzoR. In addition, the monitoring of enzymatic conversion of probe **4c** by UPLC-MS analysis (Figure 1e) confirmed the formation of fluorophore **2c** and aniline **5**, thus attesting to the complete reduction of azobenzene by AzoR undergoing the rupture of the N=N bond. All these data suggest that the selective activation of **4c** by AzoR activity leads to the release of the fluorophore **2c**, which can be further observed using fluorescence microscopy. To investigate this, we conducted confocal imaging experiments in live A549 lung cancer cells. The fluorophores **2a-f** were first evaluated for their toxicity on A549 human cells (Cf. Figure S13), and then, incubated at a non-toxic concentration for 3 h. Co-localization experiments in confocal microscopy using MitoVew™ 633 confirmed the ability of **2b** and **2c** to accumulate in mitochondria (Cf. Figures S16 and S17). Note that prolonged illumination tends to induce the translocation of fluorophores **2b** and **2c** respectively from mitochondria to the plasmic membrane (Figure S21) or the nucleus (Figure S22). This phenomenon might be attributed to the production of ROS by the fluorophore in the excited state. As already observed in previous studies,[60] This, can induce depolarization of the mitochondrial double membrane, and result in the fluorophore's exit. We also observed in live cell microscopy experiments a better signal quality with non-targeted fluorophores **2a** and **2e**, suggesting their better cell permeability. (See Figures S15 and S19). As expected, none of these two dyes accumulated in the organelle, supporting their use as non-mitochondria-targeted control compounds. We then selected a set of azo-based probes for further studies, based on their solubility, the ability of their fluorophore to penetrate the cell, and their response to AzoR during in vitro assays. Two mito-targeted probes (**4b** and **4c**) were thus selected as well as the non-targeted control probe **4e**. These probes were incubated at non-toxic concentrations (Cf Figure S14) with A549 human cells. As we can see in Figure 2a, no fluorescent signal was detected with the non-mitochondrial-targeted probe **4e**, indicating the absence of activation occurring outside the mitochondria. In contrast, incubation of the pyridinium-bearing probe **4c** resulted in the appearance of a strong green fluorescent signal within a few hours, and this at a low sub-micromolar concentration. Co-localization experiments performed with a NIR mitochondrial marker (MitoView™ 633) confirmed that activation of the **4c** probe had indeed occurred within mitochondria.

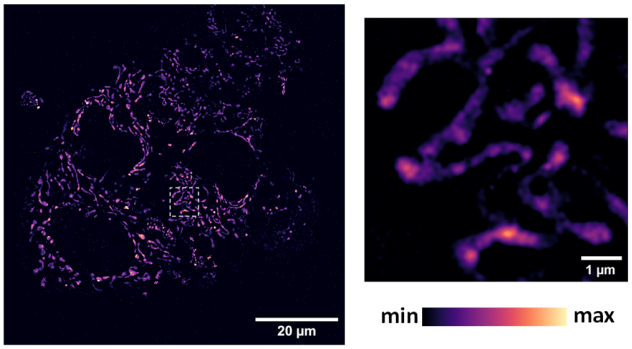

Figure 3. SIM high-resolution imaging of mitochondrial AzoR in living cells. A459 live cells were incubated for 2 h with probe **2c** at 0.5 µM (λExc: 405 nm). Emission recorded using a multi Band-Pass filter (495-550nm, 570-620nm)

This was undoubtedly confirmed by the plot profile experiment (Figure 2b) and Van Steensel Cross-correlation functions (Figure 2c). We then recorded the emission spectrum of the signal resulting from the activation of probe **4c** in the cell and compared it with the one acquired with the native fluorophore **2c**.The excellent overlap between the two emission spectra displayed in Figure 2d demonstrates the nature of the released fluorophore, and by extension, the intra-mitochondrial cleavage of the N=N double bond. In addition, two control experiments conducted with markers for the lysosome (Figure S23) and nucleus (Figure S24) confirmed the absence of signal in these two compartments of the cell. However, a very low and almost undetectable signal was observed with mito-targeted probe **4b**. In our opinion, this may be attributed to the deleterious contributions of both low solubility and partial inhibition of enzymatic activity, as observed in the *in vitro* tests. This example contributes to warning on the fact that the effectiveness of the TPP motif in targeting mitochondria may not be systematic and should be considered with caution. We also performed structured illumination microscopy (SIM) using probe **2c.**

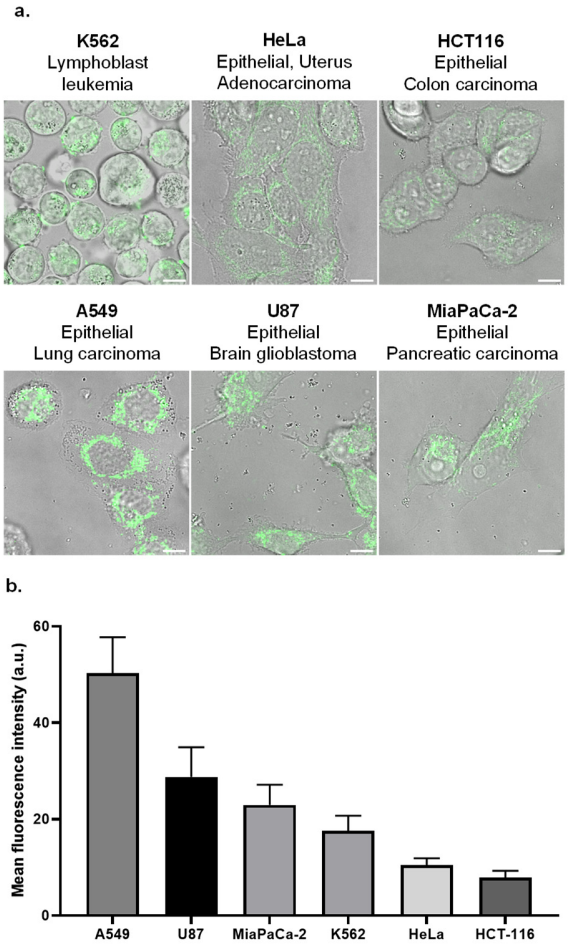

Figure 4. Variation in mitochondrial AzoR expression in different cell lines. **a.** Confocal microscopy experiments in different cell lines with Azo probe **4c** (0.5 µM). (λExc: 440 nm, λEm: 450 to 550 nm), Scale bar: 10 µm. **b.** Fluorescence intensity measured in different regions of interest of the same size in mitochondria from different cell lines with average values calculated with n = 10 measurements (See Table S3).

The high resolution images displayed in Figure 3 provides clear evidence of a signal exclusively contained in mitochondria, attesting once again to the intra-mitochondrial nature of probe activation by AzoR activity.

In summary, using probe **4c** we observed here a non-oxygen-sensitive intramitochondrial azoreductase activity, which is the first evidence of mitochondrial AzoR activity under normoxic conditions.This important discovery led us to investigate the possible extension of this biochemical process in multiple cell lines. We, therefore, replicated this imaging experiment on multiple cell lines, while strictly maintaining the same acquisition parameters during the confocal microscopy equipment. The images displayed in figure 4a were acquired after incubation with the same batch of probe **4c** under identical conditions (concentration, time, temperature) so that the results obtained can be compared. This experiment showed systematic activation of the probe. However, variable fluorescence intensities were observed reflecting a fluctuating degree of activation. This suggests different levels intramitochondrial AzoR activity according to the cell line. Nevertheless, these data should be cautiously considered. AzoR activity with different substrate specificity and the relative ability of probe **4c** to penetrate the different types of cells may also be contributing factors to the variation in fluorescence signal.

CONCLUSION

In conclusion, this work reveals for the first time the presence of an endogenous mitochondrial Azoreductase activity operating under normoxic conditions. To our knowledge, no existing study has ever evidenced the intramitochondrial metabolism of azobenzenes by rupture of the N=N double bond. In the future, this natural metabolism of azobenzenes could inspire researchers to develop new therapeutic strategies, through the production of pro-drugs, as has already been proposed with other enzymatic activities such as nitroreductase. The observed differential expression of this enzymatic activity depending on the cell line, could offer prospects for cell differentiation. In our opinion, this is a breakthrough that contributes to a better understanding of the functioning of mitochondria, a cellular organelle now considered a key target for multiple therapeutic strategies

ASSOCIATED CONTENT

Supporting Information. Figures S1-S24 and Tables S1-S3, detailed synthetic procedures and analytical data of presented compounds, NMR and HRMS spectra, “This material is available free of charge via the Internet at http://pubs.acs.org.”

AUTHOR INFORMATION

Corresponding Author

* **Arnaud Chevalier** – Université Paris-Saclay, CNRS, Institut de Chimie des Substances Naturelles, UPR 2301, 91198, Gif-sur-Yvette, France. https://orcid.org/0000-0002-0452-1554; Email : arnaud.chevalier@cnrs.fr.

Authors

The manuscript was written through contributions of all authors. / All authors have given approval to the final version of the manuscript

Laurane Michel - *Université Paris-Saclay, CNRS, Institut de Chimie des Substances Naturelles, UPR 2301, 91198, Gif-sur-Yvette, France*

Marie Auvray - *CNRS UMR 9187, Inserm U1196 Chemistry and Modeling for the Biology of Cancer Institut Curie,Université PSL 91400 Orsay (France) - CNRS UMR 9187, Inserm U1196 Chemistry and Modeling for the Biology of Cancer Université Paris-Saclay 91400 Orsay (France)*

Laurie Askenatzis – **-** *Université Paris-Saclay, CNRS, Institut de Chimie des Substances Naturelles, UPR 2301, 91198, Gif-sur-Yvette, France*

Marie-Ange Badet-Denisot - *Université Paris-Saclay, CNRS, Institut de Chimie des Substances Naturelles, UPR 2301, 91198, Gif-sur-Yvette, France*

Jérôme Bignon - *Université Paris-Saclay, CNRS, Institut de Chimie des Subs-tances Naturelles, UPR 2301, 91198, Gif-sur-Yvette, France*

Philippe Durand - *Université Paris-Saclay, CNRS, Institut de Chimie des Substances Naturelles, UPR 2301, 91198, Gif-sur-Yvette, France.*

Florence Mahuteau-Betzer –*CNRS UMR 9187, Inserm U1196 Chemistry and Model-ing for the Biology of Cancer Institut Curie,Université PSL 91400 Orsay (France) - CNRS UMR 9187, Inserm U1196 Chemistry and Modeling for the Biology of Cancer Université Paris-Saclay, 91400 Orsay (France)*

ACKNOWLEDGMENT

This project has received funding by the French National Research Agency under the program ANR-21-CE18-0005-01 grant. This work has also been supported as part of France 2030 programme "ANR-11-IDEX-0003". We also thank the Institut de Chimie des Substances Naturelles for their financial support. The present work has benefited from the Imagerie-Gif light microscopy core facility supported by the French National Research Agency (ANR-11-EQPX-0029/Morphoscope, ANR-10-INBS-04/FranceBioImaging; ANR-11-IDEX-0003-02/Saclay Plant Sciences). Université Paris-Saclay and the CNRS are also acknowledged.

ABBREVIATIONS

AzoR, Azoreductase; BSA, Bovin Serum Albumin; PBS, Phosphate buffer saline; NTR, Nitroreductase; SIM, Structure Illumination Microscopy; TPP, Triphenylphosphonium; UPLC-MS, Ultra Performance Liquid Chromatography-Mass Spectrometry

REFERENCES

1. Murphy, M. P.; Hartley, R. C., Mitochondria as a therapeutic target for common pathologies. *Nat. Rev. Drug. Discov.* **2018,** *17* (12), 865-886.
2. Scheid, A. D.; Beadnell, T. C.; Welch, D. R., Roles of mitochondria in the hallmarks of metastasis. *Br. J. Cancer* **2021,** *124* (1), 124-135.
3. Vyas, S.; Zaganjor, E.; Haigis, M. C., Mitochondria and Cancer. *Cell* **2016,** *166* (3), 555-566.
4. Wallace, D. C., Mitochondria and cancer. *Nat. Rev. Cancer.* **2012,** *12* (10), 685-98.
5. Golpich, M.; Amini, E.; Mohamed, Z.; Azman Ali, R.; Mohamed Ibrahim, N.; Ahmadiani, A., Mitochondrial Dysfunction and Biogenesis in Neurodegenerative diseases: Pathogenesis and Treatment. *CNS Neurosci. Ther.* **2017,** *23* (1), 5-22.
6. Lin, M. T.; Beal, M. F., Mitochondrial dysfunction and oxidative stress in neurodegenerative diseases. *Nature* **2006,** *443* (7113), 787-95.
7. Monzio Compagnoni, G.; Di Fonzo, A.; Corti, S.; Comi, G. P.; Bresolin, N.; Masliah, E., The Role of Mitochondria in Neurodegenerative Diseases: the Lesson from Alzheimer's Disease and Parkinson's Disease. *Mol. Neurobiol.* **2020,** *57* (7), 2959-2980.
8. Wang, Y.; Xu, E.; Musich, P. R.; Lin, F., Mitochondrial dysfunction in neurodegenerative diseases and the potential countermeasure. *CNS Neurosci. Ther.* **2019,** *25* (7), 816-824.

9. Szendroedi, J.; Phielix, E.; Roden, M., The role of mitochondria in insulin resistance and type 2 diabetes mellitus. *Nat. Rev. Endocrinol.* **2011,** *8* (2), 92-103.
10. Li, Y.-f.; Xie, Z.-f.; Song, Q.; Li, J.-y., Mitochondria homeostasis: Biology and involvement in hepatic steatosis to NASH. *Acta Pharmacol. Sin.* **2022,** *43* (5), 1141-1155.
11. Bonora, M.; Wieckowski, M. R.; Sinclair, D. A.; Kroemer, G.; Pinton, P.; Galluzzi, L., Targeting mitochondria for cardiovascular disorders: therapeutic potential and obstacles. *Nat. Rev. Cardiol.* **2019,** *16* (1), 33-55.
12. Ramachandran, K.; Maity, S.; Muthukumar, A. R.; Kandala, S.; Tomar, D.; Abd El-Aziz, T. M.; Allen, C.; Sun, Y.; Venkatesan, M.; Madaris, T. R.; Chiem, K.; Truitt, R.; Vishnu, N.; Aune, G.; Anderson, A.; Martinez-Sobrido, L.; Yang, W.; Stockand, J. D.; Singh, B. B.; Srikantan, S.; Reeves, W. B.; Madesh, M., SARS-CoV-2 infection enhances mitochondrial PTP complex activity to perturb cardiac energetics. *iScience* **2022,** *25* (1), 103722.
13. Smith, R. A. J.; Porteous, C. M.; Gane, A. M.; Murphy, M. P., Delivery of bioactive molecules to mitochondria in vivo. *Proc. Natl. Acad. Sci. U.S.A.* **2003,** *100* (9), 5407-5412.
14. Murphy, M. P., Selective targeting of bioactive compounds to mitochondria. *Trends Biotechnol.* **1997,** *15* (8), 326-330.
15. Zielonka, J.; Joseph, J.; Sikora, A.; Hardy, M.; Ouari, O.; Vasquez-Vivar, J.; Cheng, G.; Lopez, M.; Kalyanaraman, B., Mitochondria-Targeted Triphenylphosphonium-Based Compounds: Syntheses, Mechanisms of Action, and Therapeutic and Diagnostic Applications. *Chem. Rev.* **2017,** *117* (15), 10043-10120.
16. Rin Jean, S.; Tulumello, D. V.; Wisnovsky, S. P.; Lei, E. K.; Pereira, M. P.; Kelley, S. O., Molecular vehicles for mitochondrial chemical biology and drug delivery. *ACS Chem. Biol.* **2014,** *9* (2), 323-33.
17. Wang, H.; Fang, B.; Peng, B.; Wang, L.; Xue, Y.; Bai, H.; Lu, S.; Voelcker, N. H.; Li, L.; Fu, L.; Huang, W., Recent Advances in Chemical Biology of Mitochondria Targeting. *Front. Chem.* **2021,** *9*, 683220.
18. Roopa; Kumar, N.; Bhalla, V.; Kumar, M., Development and sensing applications of fluorescent motifs within the mitochondrial environment. *Chem. Commun.* **2015,** *51* (86), 15614-28.
19. Xu, Z.; Xu, L., Fluorescent probes for the selective detection of chemical species inside mitochondria. *Chem. Commun.* **2016,** *52* (6), 1094-119.
20. Samanta, S.; He, Y.; Sharma, A.; Kim, J.; Pan, W.; Yang, Z.; Li, J.; Yan, W.; Liu, L.; Qu, J.; Kim, J. S., Fluorescent Probes for Nanoscopic Imaging of Mitochondria. *Chem* **2019,** *5* (7), 1697-1726.
21. Scalcon, V.; Bindoli, A.; Rigobello, M. P., Significance of the mitochondrial thioredoxin reductase in cancer cells: An update on role, targets and inhibitors. *Free Radic. Biol. Med.* **2018,** *127*, 62-79.
22. Kameritsch, P.; Singer, M.; Nuernbergk, C.; Rios, N.; Reyes, A. M.; Schmidt, K.; Kirsch, J.; Schneider, H.; Müller, S.; Pogoda, K.; Cui, R.; Kirchner, T.; de Wit, C.; Lange-Sperandio, B.; Pohl, U.; Conrad, M.; Radi, R.; Beck, H., The mitochondrial thioredoxin reductase system (TrxR2) in vascular endothelium controls peroxynitrite levels and tissue integrity. *Proc. Natl. Acad. Sci. U.S.A.* **2021,** *118* (7), e1921828118.
23. Conrad, M.; Jakupoglu, C.; Moreno, S. G.; Lippl, S.; Banjac, A.; Schneider, M.; Beck, H.; Hatzopoulos, A. K.; Just, U.; Sinowatz, F.; Schmahl, W.; Chien, K. R.; Wurst, W.; Bornkamm, G. W.; Brielmeier, M., Essential Role for Mitochondrial Thioredoxin Reductase in Hematopoiesis, Heart Development, and Heart Function. *Mol. Cell. Biol.* **2004,** *24* (21), 9414-9423.
24. Cabreiro, F.; Picot, C. R.; Perichon, M.; Castel, J.; Friguet, B.; Petropoulos, I., Overexpression of Mitochondrial Methionine Sulfoxide Reductase B2 Protects Leukemia Cells from Oxidative Stress-induced Cell Death and Protein Damage*. *J. Biol. Chem.* **2008,** *283* (24), 16673-16681.
25. Lee, M. H.; Han, J. H.; Lee, J. H.; Choi, H. G.; Kang, C.; Kim, J. S., Mitochondrial thioredoxin-responding off-on fluorescent probe. *J. Am. Chem. Soc.* **2012,** *134* (41), 17314-9.
26. Liu, Y.; Ma, H.; Zhang, L.; Cui, Y.; Liu, X.; Fang, J., A small molecule probe reveals declined mitochondrial thioredoxin reductase activity in a Parkinson's disease model. *Chem. Commun.* **2016,** *52* (11), 2296-9.
27. Mafireyi, T. J.; Escobedo, J. O.; Strongin, R. M., Fluorogenic probes for thioredoxin reductase activity. *Results Chem.* **2021,** *3*, 100127.
28. Yang, Y. P.; Qi, F. J.; Zheng, Y. L.; Duan, D. C.; Bao, X. Z.; Dai, F.; Zhang, S.; Zhou, B., Fast Imaging of Mitochondrial Thioredoxin Reductase Using a Styrylpyridinium-Based Two-Photon Ratiometric Fluorescent Probe. *Anal. Chem.* **2022,** *94* (12), 4970-4978.
29. Chevalier, A.; Zhang, Y.; Khdour, O. M.; Kaye, J. B.; Hecht, S. M., Mitochondrial Nitroreductase Activity Enables Selective Imaging and Therapeutic Targeting. *J. Am. Chem. Soc.* **2016,** *138* (37), 12009-12.
30. Huang, B.; Chen, W.; Kuang, Y. Q.; Liu, W.; Liu, X. J.; Tang, L. J.; Jiang, J. H., A novel off-on fluorescent probe for sensitive imaging of mitochondria-specific nitroreductase activity in living tumor cells. *Org. Biomol. Chem.* **2017,** *15* (20), 4383-4389.
31. Thiel, Z.; Rivera-Fuentes, P., Single-Molecule Imaging of Active Mitochondrial Nitroreductases Using a Photo-Crosslinking Fluorescent Sensor. *Angew. Chem. Int. Ed. Engl.* **2019,** *58* (33), 11474-11478.
32. Safir Filho, M.; Dao, P.; Martin, A. R.; Benhida, R., Nitroreductase sensitive styryl-benzothiazole profluorescent probes for the visualization of mitochondria under normoxic conditions. *J. Photochem. Photobiol. A: Chem.* **2020,** *396*, 112528.
33. Zhu, N.; Xu, G.; Wang, R.; Zhu, T.; Tan, J.; Gu, X.; Zhao, C., Precise imaging of mitochondria in cancer cells by real-time monitoring of nitroreductase activity with a targetable and activatable fluorescent probe. *Chem. Commun.* **2020,** *56* (56), 7761-7764.
34. Wang, S.; Tan, W.; Lang, W.; Qian, H.; Guo, S.; Zhu, L.; Ge, J., Fluorogenic and Mitochondria-Localizable Probe Enables Selective Labeling and Imaging of Nitroreductase. *Anal. Chem.* **2022,** *94* (20), 7272-7277.
35. Nguyen, J.; Tirla, A.; Rivera-Fuentes, P., Disruption of mitochondrial redox homeostasis by enzymatic activation of a trialkylphosphine probe. *Org. Biomol. Chem.* **2021,** *19* (12), 2681-2687.
36. Shin, W. S.; Lee, M. G.; Verwilst, P.; Lee, J. H.; Chi, S. G.; Kim, J. S., Mitochondria-targeted aggregation induced emission theranostics: crucial importance of in situ activation. *Chem. Sci.* **2016,** *7* (9), 6050-6059.
37. Yuan, Z.; Xu, M.; Wu, T.; Zhang, X.; Shen, Y.; Ernest, U.; Gui, L.; Wang, F.; He, Q.; Chen, H., Design and synthesis of NQO1 responsive fluorescence probe and its application in bio-imaging for cancer diagnosis. *Talanta* **2019,** *198*, 323-329.
38. Yang, Y. P.; Qi, F. J.; Qian, Y. P.; Bao, X. Z.; Zhang, H. C.; Ma, B.; Dai, F.; Zhang, S. X.; Zhou, B., Developing Push-Pull Hydroxylphenylpolyenylpyridinium Chromophores as Ratiometric Two-Photon Fluorescent Probes for Cellular and Intravital Imaging of Mitochondrial NQO1. *Anal. Chem.* **2021,** *93* (4), 2385-2393.
39. Xiang, M. H.; Huang, H.; Liu, X. J.; Tong, Z. X.; Zhang, C. X.; Wang, F.; Yu, R. Q.; Jiang, J. H., Mitochondrion-Targeting Fluorescence Probe via Reduction Induced Charge Transfer for Fast Methionine Sulfoxide Reductases Imaging. *Anal. Chem.* **2019,** *91* (9), 5489-5493.
40. Saratale, R. G.; Saratale, G. D.; Chang, J. S.; Govindwar, S. P., Bacterial decolorization and degradation of azo dyes: A review. *J. Taiwan Inst. Chem.* **2011,** *42* (1), 138-157.
41. Tian, Y.; Li, Y.; Jiang, W.-L.; Zhou, D.-Y.; Fei, J.; Li, C.-Y., In-Situ Imaging of Azoreductase Activity in the Acute and Chronic Ulcerative Colitis Mice by a Near-Infrared Fluorescent Probe. *Anal. Chem.* **2019,** *91* (16), 10901-10907.
42. Rattray, N. J. W.; Zalloum, W. A.; Mansell, D.; Latimer, J.; Schwalbe, C. H.; Blake, A. J.; Bichenkova, E. V.; Freeman, S., Fluorescent probe for detection of bacteria: conformational trigger upon bacterial reduction of an azo bridge. *Chem. Commun.* **2012,** *48* (51), 6393-6395.
43. Chevalier, A.; Mercier, C.; Saurel, L.; Orenga, S.; Renard, P.-Y.; Romieu, A., The first latent green fluorophores for the detection of azoreductase activity in bacterial cultures. *Chem. Commun.* **2013,** *49* (78), 8815-8817.

44. Tian, X.; Li, Z.; Sun, Y.; Wang, P.; Ma, H., Near-Infrared Fluorescent Probes for Hypoxia Detection via Joint Regulated Enzymes: Design, Synthesis, and Application in Living Cells and Mice. *Anal. Chem.* **2018,** *90* (22), 13759-13766.

45. Ma, D.; Huang, C.; Zheng, J.; Zhou, W.; Tang, J.; Chen, W.; Li, J.; Yang, R., Azoreductase-Responsive Nanoprobe for Hypoxia-Induced Mitophagy Imaging. *Anal. Chem.* **2019,** *91* (2), 1360-1367.

46. Guo, L.; Zhuge, Y.; Yang, L.; Qiu, H.; Liu, J.; Wang, P., A two-photon mitochondria-targeting azo reductase probe for imaging in tumor cells and mice. *DyesPigm.* **2023,** *218*, 111512.

47. Chevalier, A.; Renard, P.-Y.; Romieu, A., Azo-Based Fluorogenic Probes for Biosensing and Bioimaging: Recent Advances and Upcoming Challenges. *Chem. Asian J.* **2017,** *12* (16), 2008-2028.

48. Guisan-Ceinos, S.; A, R. R.; Romeo-Gella, F.; Simon-Fuente, S.; Gomez-Pastor, S.; Calvo, N.; Orrego, A. H.; Guisan, J. M.; Corral, I.; Sanz-Rodriguez, F.; Ribagorda, M., Turn-on Fluorescent Biosensors for Imaging Hypoxia-like Conditions in Living Cells. *J. Am. Chem. Soc.* **2022,** *144* (18), 8185-8193.

49. Geraghty, C.; Wynne, C.; Elmes, R. B. P., 1,8-Naphthalimide based fluorescent sensors for enzymes. *Coord. Chem. Rev.* **2021,** *437*, 213713.

50. Jain, N.; Kaur, N., A comprehensive compendium of literature of 1,8-Naphthalimide based chemosensors from 2017 to 2021. *Coord. Chem. Rev.* **2022,** *459*, 214454.

51. Liu, H.-W.; Xu, S.; Wang, P.; Hu, X.-X.; Zhang, J.; Yuan, L.; Zhang, X.-B.; Tan, W., An efficient two-photon fluorescent probe for monitoring mitochondrial singlet oxygen in tissues during photodynamic therapy. *Chem. Commun.* **2016,** *52* (83), 12330-12333.

52. Bagale, S. M.; Brown, A. S.; Carballosa Gonzalez, M. M.; Vitores, A.; Micotto, T. L.; Saleesh Kumar, N. S.; Hentall, I. D.; Wilson, J. N., Fluorescent reporters of monoamine transporter distribution and function. *Bioorg. Med. Chem. Lett.* **2011,** *21* (24), 7387-7391.

53. Yuan, D.; Brown, R. G.; Hepworth, J. D.; Alexiou, M. S.; Tyman, J. H. P., The synthesis and fluorescence of novel N-substituted-1,8-naphthylimides. *J. Heterocycl. Chem.* **2008,** *45* (2), 397-404.

54. Wojciechowski, K., Spectrophotometric characteristics of N,N-dialkylamino-3- and 4-phenylazonaphthalimides. *Dyes Pigm.* **1988,** *9* (6), 401.

55. Bandara, H. M. D.; Burdette, S. C., Photoisomerization in different classes of azobenzene. *Chem. Soc. Rev.* **2012,** *41* (5), 1809-1825.

56. Guisán-Ceinos, S.; R. Rivero, A.; Romeo-Gella, F.; Simón-Fuente, S.; Gómez-Pastor, S.; Calvo, N.; Orrego, A. H.; Guisán, J. M.; Corral, I.; Sanz-Rodriguez, F.; Ribagorda, M., Turn-on Fluorescent Biosensors for Imaging Hypoxia-like Conditions in Living Cells. *J. Am. Chem. Soc.* **2022,** *144* (18), 8185-8193.

57. Pauli, J.; Vag, T.; Haag, R.; Spieles, M.; Wenzel, M.; Kaiser, W. A.; Resch-Genger, U.; Hilger, I., An in vitro characterization study of new near infrared dyes for molecular imaging. *Eur. J. Med. Chem.* **2009,** *44* (9), 3496-3503.

58. Nakanishi, M.; Yatome, C.; Ishida, N.; Kitade, Y., Putative ACP Phosphodiesterase Gene (acpD) Encodes an Azoreductase *. *J. Biol. Chem.* **2001,** *276* (49), 46394-46399.

59. Boulègue, C.; Löweneck, M.; Renner, C.; Moroder, L., Redox Potential of Azobenzene as an Amino Acid Residue in Peptides. *ChemBioChem* **2007,** *8* (6), 591-594.

60. Chennoufi, R.; Bougherara, H.; Gagey-Eilstein, N.; Dumat, B.; Henry, E.; Subra, F.; Mahuteau-Betzer, F.; Tauc, P.; Teulade-Fichou, M. P.; Deprez, E., Differential behaviour of cationic triphenylamine derivatives in fixed and living cells: triggering and imaging cell death. *Chem. Commun.* **2015,** *51* (80), 14881-14884.